J. Fluid Mech. (1965), *vol.* 23, *part* 2, *pp.* 325–335
Printed in Great Britain

Static menisci on the outside of cylinders

By D. A. WHITE† AND J. A. TALLMADGE‡
Department of Engineering and Applied Science, Yale University, New Haven, Conn.

(Received 25 February 1965)

The Laplace equation for the pressure drop across curved liquid-gas interfaces is applied to the solution of the profile of a static liquid meniscus on the outside of a wire of circular cross-section. The resulting differential equation is integrated numerically, an operation complicated by the existence of boundary conditions at two points making a trial-and-error solution necessary. The accuracy of the solution is substantiated by comparison of computed profiles with experiments in which menisci of a blue dye in water are photographed clinging to the outside of brass wires, whose diameters lie within the range of technological interest.

1. Introduction

The authors are studying the films of liquids adhering to cylinders withdrawn from baths of quiescent liquids. A rational theory for the liquid film on a non-horizontal flat plate has been given by Landau & Levich (1942). This theory involves the knowledge of the value of the second derivative of the meniscus profile at its highest point on the flat plate. In order to extend Landau & Levich's theory to wires of any radius it is necessary to have computed profiles of their menisci from which the value of the required second derivative can be calculated.

The profile of the liquid meniscus on a flat plate has been known for some time and is given in several textbooks, e.g. Levich (1962). The maximum height of liquid on the meniscus and the second derivative at this point are also given by Levich. This solution assumes perfect wetting of the solid by the liquid, that is to say that the angle of contact is zero. This will be assumed in the subsequent development.

The flat plate profile was derived from the Laplace equation (equation (1) below), which may be integrated easily for two-dimensional problems. Cases exhibiting axial symmetry present more difficulties. Several solutions are, however, presented by Adam (1938); they allow the calculation of precise corrections for surface-tension measurements. The profile of a cylindrical meniscus has not been calculated previously, although a discussion of the problem appears in the work of Bondarenko (1948).

It is the purpose of this work to predict the profile of a meniscus on a vertical wire as a function of wire radius (R) and fluid properties by numerical integration

† Present address: Department of Chemical Engineering, Cambridge University.
‡ Present address: Department of Mechanical Engineering, Imperial College of Science and Technology, London.

The pressure change Δp is balanced by the hydrostatic pressure due to gravity. Thus $\Delta p = -\rho g x$, where ρ is the fluid density and g the acceleration due to gravity. Consequently

$$d^2s/dx^2 = [1+(ds/dx)^2][(\rho g x/\sigma)\{1+(ds/dx)^2\}^{\frac{1}{2}}+1/s]. \tag{5}$$

The two boundary conditions are

$$ds/dx = 0 \quad \text{at} \quad x = b, \tag{6}$$

and

$$d^2s/dx^2 \to \infty \quad \text{at} \quad x = 0. \tag{7}$$

The first, (6), represents a zero wetting angle. On the free surface at $x = 0$, s, s' and s'' are clearly infinite so that any one might be used for the second boundary condition. Since numerical integration showed that $s'' > s' > s$ as $x \to 0$, the second derivative was chosen for the second boundary condition and was used as a criterion of the approach of the solution to infinity. These boundary conditions constitute a 'two-point' problem (Hamming 1962, p. 219), adding further complexities to the problem.

Equation (5) can be made dimensionless by use of a liquid property, the capillary length a, where

$$a = (2\sigma/\rho g)^{\frac{1}{2}}. \tag{8}$$

Defining dimensionless co-ordinates $X = x/a$ and $S = s/a$, equation (5) becomes

$$d^2S/dX^2 = [1+(dS/dX)^2][2X\{1+(dS/dX)^2\}^{\frac{1}{2}}+1/S]. \tag{9}$$

The two point boundary conditions (6) and (7) can be written in dimensionless form

$$dS/dX = 0 \quad \text{at} \quad X = B, \tag{10}$$

$$d^2S/dX^2 \to \infty \quad \text{at} \quad X = 0, \tag{11}$$

where $B = b/a$, the normalized maximum height. Using the dimensionless wire radius of Gutfinger & Tallmadge (1964), $G_0 = R/a$, the co-ordinates of the point on the highest part of the meniscus ($x = b$ at $s = R$ in figure 1) are

$$X = B \quad \text{at} \quad S = G_0. \tag{12}$$

At this point $dS/dX = 0$; consequently (9) becomes

$$(d^2S/dX^2)_B = 2B + 1/G_0. \tag{13}$$

By differentiation of (9), and substitution of $dS/dX = 0$, we obtain the value of the third derivative at B, which is

$$(d^3S/dX^3)_B = 2. \tag{14}$$

The expressions (9) to (14) give us the equations, boundary conditions and derivatives in the form in which they are used in the subsequent numerical integration. However, before describing this integration a special case of equation (9) should be mentioned: the flat plate, where $R \to \infty$ or $G_0 \to \infty$. In this case we have $S \to \infty$ for all portions of the meniscus and equation (9) becomes, where $H = (s-R)/a$,

$$d^2H/dX^2 = 2X\{1+(dH/dX)^2\}^{\frac{3}{2}}. \tag{15}$$

Since $B = 1$ for a flat plate, the first boundary condition is

$$dH/dX = 0 \quad \text{at} \quad X = 1, \tag{16}$$

and the second remains as (11). The equation may be integrated twice to give the meniscus profile as

$$H = 2^{-\frac{1}{2}} \cosh^{-1}[(\sqrt{2})/X] - (2-X)^{\frac{1}{2}} + 0{\cdot}377, \tag{17}$$

which is given by Landau & Lifshitz (1959). The case where the contact angle is not zero is also discussed by Landau & Lifshitz (1959).

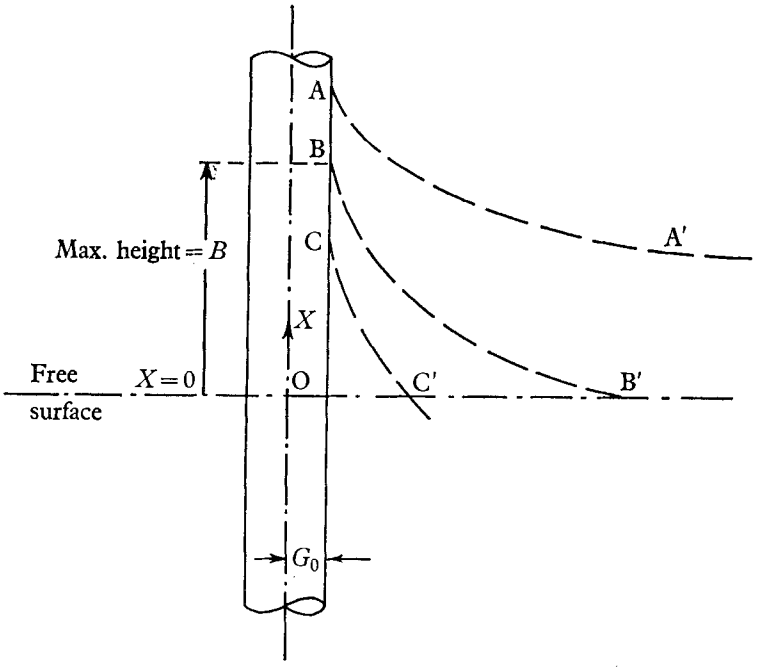

FIGURE 2. Trial-and-error solution.

2.2. *Numerical integration*

At the start of each integration (at $X = B$), the meniscus profile and derivative was approximated by a Taylor series solution using expressions (10), (12), (13) and (14). Thus

$$S = G_0 + \tfrac{1}{2}n^2f^2[2B + 1/G_0] + \tfrac{1}{3}n^3f^3, \tag{18}$$

where f is the step size and n the number of steps before B. The integration procedure used is the 'one half' formula given by Hamming (1962, p. 207).

In order to start an integration using (18) the value of both G_0 and B are required. However, B as a function of G_0 is not known a priori, in consequence it has to be determined by a trial-and-error solution. In any case the value of B will be less than that for the case of a flat plate where $B = 1$. The trial-and-error solution is illustrated in figure 2. For a given G_0 a value of B is guessed and the numerical integration can then be started. If the value of B is too large, the computed profile will take the form shown by curve AA', with $d^2S/dX^2 \to \infty$

before $X = 0$. This second derivative was assumed infinite when its value had exceeded 10^8. On the other hand, too small a guess will result in the computation of curve CC′ which reaches $X = 0$ before $d^2S/dX^2 \to \infty$. An iteration procedure based on these two tests was incorporated in the computer programme to adjust the value of B until the resulting value of B was determined to a required degree of precision. Thus (S, X) profiles were determined simultaneously. Further details are available elsewhere (White 1965).

2·3. *Profiles and curvature*

Values of B for given G_0 are given in table 1. They were determined to within $\pm 0{\cdot}0005$, which was the criterion used for terminating the B-iteration, but are subject to truncation errors from various causes such as the series approximation

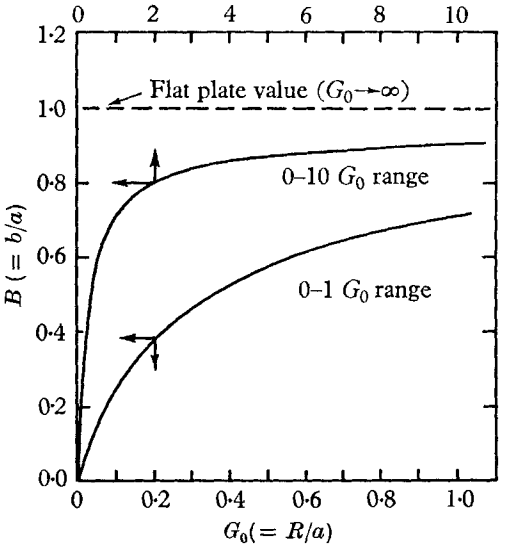

FIGURE 3. The effect of wire radius on maximum height; theory.

at the start, the second-derivative stop-criterion, or the step size. As shown in the plot of B vs G_0 (figure 3), the maximum height approaches the flat plate value as expected (i.e. $B \to 1$ as $G_0 \to \infty$) and tends to vanish as the radius of the wire approaches zero (i.e. $B \to 0$ as $G_0 \to 0$).

The values of B can be estimated using the following semi-empirical formula

$$B_E = 2{\cdot}4G_0^{0{\cdot}85}/(1 + 2{\cdot}4G_0^{0{\cdot}85}), \tag{19}$$

which holds to within $\pm 1\%$ of the computed values in the region $0{\cdot}03 < G_0 < 3{\cdot}0$, which is the region of technological interest for withdrawal (Tallmadge, Labine & Wood 1965). The form of equation (19) was suggested by the shape of figure 3, which has the appearance of the Langmuir isotherm, $B = mG_0/(1 + mG_0)$. Rearranging this, we have $\{B/(1-B)\} = mG_0$; a plot of $\log\{B/(1-B)\}$ vs $\log G_0$ resulted in a straight line whose slope was 0·85.

The error in B consequent on using formula (19) is given in table 1. The formula gives results that are too large at $G_0 > 3$ and too small at $G_0 < 0{\cdot}03$.

Once the maximum height has been determined as a function of G_0, the curvature, C, at the upper part of the meniscus may be calculated using equation (13); such values are given in table 1.

Substituting the value of B_E given by (19) into (13), we obtain the semi-empirical formula

$$C_E = \frac{4{\cdot}8G_0^{0{\cdot}85}}{1+2{\cdot}4G_0^{0{\cdot}85}} + \frac{1}{G_0}. \tag{20}$$

The last column of table 1 indicates that the error introduced by using equation (20) is 1 % or less for $G_0 < 3{\cdot}0$.

	Maximum height		Curvature at maximum height	
Wire radius G_0 or R/a	Height B or b/a	Deviation of B_E values of (19) $(B_E-B)/B$ (%)	Curvature, from (13) $C = (d^2S/dX^2)_B$	Deviation of C_E values of (20) $(C_E-C)/C$ (%)
0·006	0·036*	−10	166·7	0
0·01	0·050*	−9	100·0	0
0·03	0·110	0	33·55	0
0·06	0·180	0	17·03	0
0·1	0·252	0	10·50	0
0·2	0·381	−1	5·762	0
0·3	0·468	−1	4·269	0
0·4	0·532	0	3·564	0
0·6	0·618	−1	2·803	0
1·0	0·713	−1	2·426	−1
3·0	0·847	1	2·027	1
6·0	0·889*	3	—	—
10·0	0·907*	4	—	—
30·0	0·926*	6	—	—
∞	1·000	0	2·000	0

* Not described, within 1 %, by the semi-empirical expression (19).

TABLE 1. Predicted effect of wire radius on maximum height and curvature

Prediction of the curvature, C, is one of the main purposes of this work. Thus it is noteworthy that (20) is accurate, both in the *limit* for two special cases (for small wires of $G_0 \to 0$ where $C_E \to 1/G_0$, and for flat plates of $G_0 \to \infty$ where $C_E \to 2$) and in one of the regions of *approach* to the limit (for small wires of $G_0 \to 0$). The only region where (20) does not describe C within 1 % is that for which dynamic film thicknesses can be represented precisely by flat plate expressions (Van Rossum 1958). Even in this region of $3 < G_0 < \infty$, the maximum difference between C_E and C is 5 %; this maximum occurs near $G_0 = 30$.

There are at least eight dimensionless forms for presenting the static meniscus profiles at constant G_0. These possibilities arise since thickness may be expressed either as s or $(s-R)$ and since both thickness and height x may be made dimensionless using either a or b (capillary length or maximum height, respectively). The most convenient form for interpolation purposes was found to be $(s-R)/a$ vs x/b, or H vs X/B in dimensionless notation. The $(s-R)$ form is better than s for comparison with flat plate results and b is better than a for making height

dimensionless since distances are normalized when b is used. Comparison of plots of $(s-R)/a$ and $(s-R)/b$ (both vs x/b) indicated that the a form brought the profiles closer together.

Computed values of static meniscus profiles are shown in table 2 and figure 4 as $H = H(X/B, G_0)$. These values, expressed at even increments of X/B, were obtained from the computed output (s/a vs x/a) by smoothing calculated values

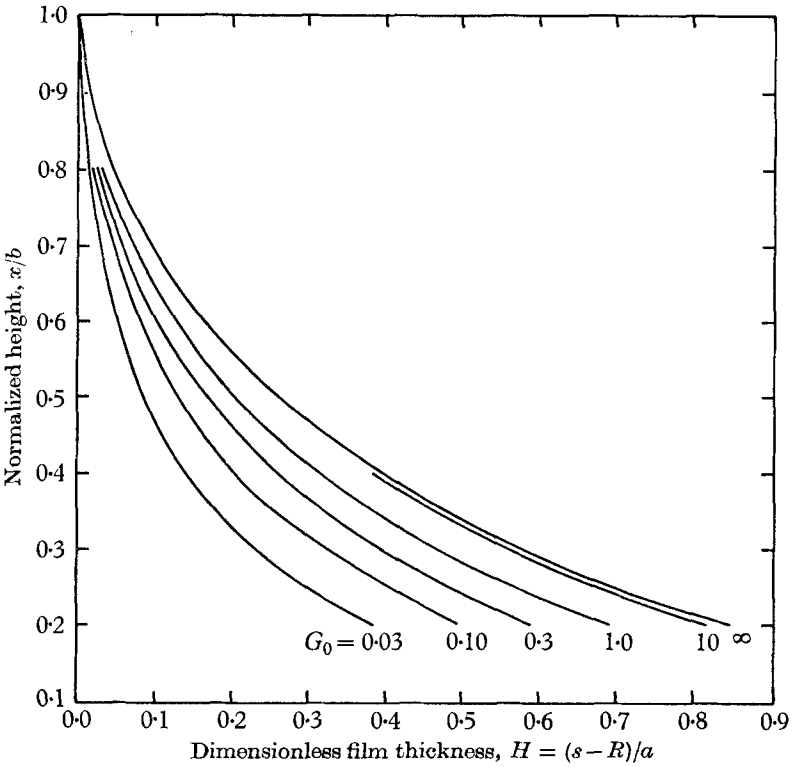

FIGURE 4. Theoretical profiles in the X/B vs H form.

$G_0(R/a)$...	0·03	0·10	0·30	1·0	10·0	∞ Flat plate*
$B(b/a)$...	0·110	0·252	0·468	0·713	0·907	1·000
X/B, or x/b						
1·0	0·0	0·0	0·0	0·0	0·0	0·0
0·9	0·003	0·005	0·006	0·008	0·009	0·010
0·8	0·008	0·015	0·019	0·027	0·036	0·039
0·7	0·022	0·039	0·050	0·067	0·084	0·087
0·6	0·044	0·076	0·097	0·122	0·154	0·158
0·5	0·078	0·126	0·163	0·200	0·247	0·256
0·4	0·136	0·197	0·253	0·312	0·382	0·388
0·3	0·226	0·321	0·390	0·462	0·560	0·575
0·2	0·380	0·494	0·590	0·693	0·817	0·846

* This column is equivalent to values from equation (17).

TABLE 2. Static meniscus profiles. Values of $H = (s-R)/a$

of H vs X/B using graphical interpolation. The graph paper was sufficiently large and the curves sufficiently smooth for the values of H reported in table 2 to be precise to the third decimal place.

Table 2 and figure 4 indicate that the thicknesses for the flat plate case represent the upper limit of those for cylinders. For the lower limit, $R \to 0$, the thicknesses tend to vanish; this is indicated by $B \to 0$ in figure 3 and by figure 4.

3. Experimental

The calculation was verified experimentally by comparing the theoretical meniscus profiles with close-up photographs of actual menisci.

3.1. *Method*

The liquid used was a 500 mg/l solution of Pontamine Blue Dye in distilled water, chosen for its dark colour and water-like properties. Water was used as it has a large capillary length and hence comparatively large menisci. Furthermore, it is one of the most sensitive fluids to surfactant agents. A diagram of the apparatus is given in figure 5. The liquid was contained in a large cylindrical

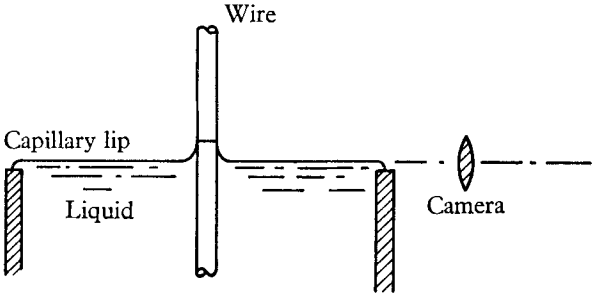

FIGURE 5. Diagram of apparatus.

vessel about 45 cm in diameter. Its temperature was held at $22{\cdot}5 \pm 0{\cdot}1$ °C. The meniscus was supported on six brass rods whose diameters varied from $\frac{1}{16}$ in. to $\frac{1}{2}$ in. ($G_0 = 0{\cdot}2$ to $1{\cdot}6$). Sizes were chosen by availability, but the G_0 range covered that value at which $C \to 1/G_0$ up to those at which thicknesses are similar to those of flat plates. The wire diameter was measured to a thousandth of an inch with a micrometer, the wires having been cleaned with chromic acid and distilled water to insure a clear wetting surface.

The capillary length a was determined by measuring the height of the liquid's rise in a glass capillary, the radius of which (0·0265 cm) was determined by calibration with benzene having $a = 0{\cdot}257$ cm. This is a direct method for measuring capillary length. The value of $0{\cdot}382 \pm 0{\cdot}001$ cm was obtained. Lange (1961) gives the following properties for pure water at 22·5 °C: $\rho = 0{\cdot}9977$ g/cm^3, $\sigma = 72{\cdot}36$ dyn/cm, and g in north-eastern United States = 980·1 cm/sec^2. These values give a value of 0·384 cm for the capillary length of pure water, compared with 0·382 cm measured for the dye solution. The closeness of these values indicated that there were no impurities in the dye solution.

The glass vessel was purposely overfilled with liquid to give a clear line of sight for the camera. A small capillary lip of liquid prevented the excess from draining down the sides of the vessel. The 35 mm camera was a single-lens 'Cannon flex' reflex camera, fitted with extension bellows on which a 45 mm 'Elmar' enlarger lens was mounted. Care was taken to mount the camera horizontally; this was done using a bubble level.

The negatives were magnified in an enlarger and the profile of meniscus and wire was traced on paper. A typical photograph is given in figure 6 (plate 1). An interesting characteristic of these shots is the existence of a reflexion of the meniscus which was formed by the liquid free surface. This image enables the position of the liquid free surface, which $X = 0$, to be determined from this picture with good accuracy. The precise scale of the enlargement was determined by measuring the width of the image of the wire.

Since lengths on the tracing were measurable to $\pm 0{\cdot}025$ cm and the magnification was about 21, precision in the measured values of $(s-R)$ and x was about $\pm 0{\cdot}0012$ cm. Measurements of the values of maximum height were not as precise due to larger location uncertainties.

Image lengths were converted directly into dimensionless co-ordinates, based on capillary length a, for comparison with theoretical calculations. Since the actual width of the wire in dimensionless co-ordinates is $2G_0$, the scale of the enlargement is thus one centimetre to $(2G_0/\text{width of image})$ dimensionless lengths. Consequently the co-ordinates of points on the meniscus were determined by multiplying measured lengths by the constant scale factor. Since, on the average, the scale of the tracings was about 1 cm to 0·1 dimensionless lengths, the lengths were precise to about $\pm 0{\cdot}0025$ dimensionless co-ordinates (H and X), assuming that there were no other errors introduced in tracing and measuring the co-ordinates. Further details are available elsewhere (White 1965).

3·2. *Results and discussion*

Experimental maximum heights for the six wires studied are compared with theory in dimensionless B form, as shown in table 3. The theoretical values, both of height and of the profiles presented below, were determined by numerical integration for the G_0 numbers given in table 3; however, B values calculated from equation (19) and H values interpolated from table 2 are equivalent.

If the profile data were plotted as X/B vs H, as in figure 4, there would be considerable crowding and overlapping of the data for each wire in the 0·2 to 1·7 range of G_0 studied. To avoid overlapping, experimental meniscus profiles are compared with theory in X vs S form (see figure 7). No experimental values of curvature at the maximum height were calculated since determinations of such second derivatives from data would be extremely sensitive to random error. It was felt, however, that confirmation of theoretical profiles and heights would imply the validity of curvature values predicted.

Replicate profile runs are plotted in figure 7 for each of the three largest wires to indicate reproducibility of results. The reproducibility with the wires of $G_0 = 1{\cdot}65$ and $0{\cdot}616$ is well within experimental precision and is very good, but one of the triplicate runs for the wire of $G_0 = 0{\cdot}830$ is not so satisfactory.

As shown in figure 7, the theory predicts profiles which agree very closely with experiment for the largest and the two smallest wires ($G_0 = 1{\cdot}65$, $0{\cdot}319$, and $0{\cdot}204$) but deviates from the experimental values in the case of the two other wires. This deviation is especially noticeable at the lower part of the meniscus where differences as large as $\pm 0{\cdot}007$ dimensionless co-ordinates are noted. How-

Wire no.	Wire radius		Maximun height, $B = b/a$	
	R(cm)	$G_0(R/a)$	Theory	Experiment
1	0·079	0·204	0·383	0·395
2	0·122	0·318	0·475	0·50
3	0·156	0·403	0·507	0·52, 0·53
4	0·237	0·616	0·612	0·615, 0·595
5	0·319	0·83	0·670	0·65, 0·65, 0·68
6	0·632	1·65	0·785	0·80, 0·83

TABLE 3. Maximum heights

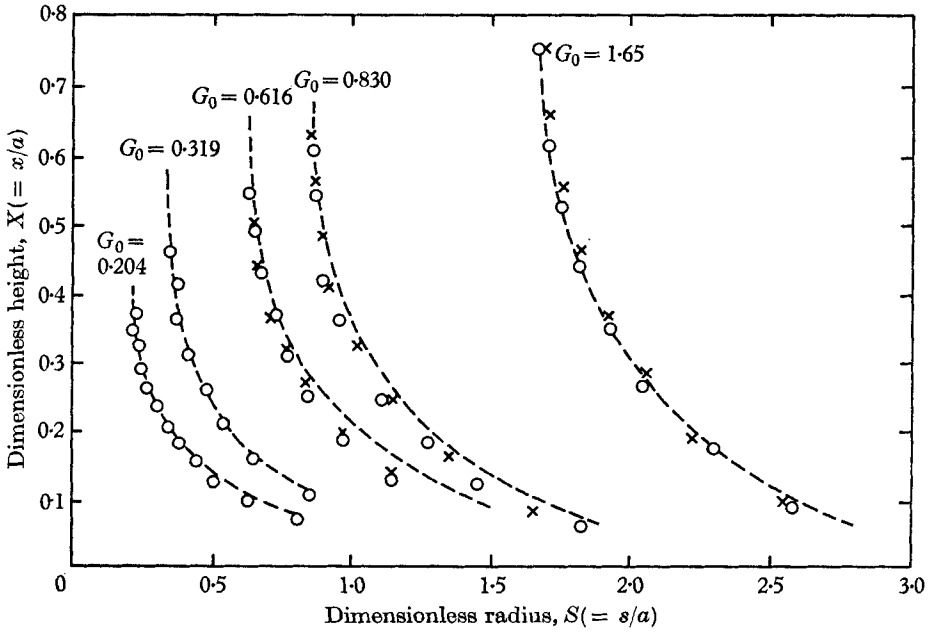

FIGURE 7. Comparison of theory with experimental profiles.

ever, at the higher region of the meniscus, the theoretical lines for these two wires ($G_0 = 0{\cdot}616$ and $0{\cdot}830$) tend towards the experimental points. In addition, a good estimate of maximum meniscus height B was given from the photographs for the two wires under discussion.

Since the profile of the meniscus is tangential to the wire at its upper point, the position of this point and the meniscus height B are difficult to measure precisely from the photographs. The meniscus-calculated values for these two wires further substantiate the accuracy of the computations described previously.

The deviations that are observed from theory are more marked at the lower portions of the meniscus, where the actual contrast and sharpness of the interface (figure 6, plate 1) is not very satisfactory. This lack of contrast is believed to explain the deviations observed in some of the runs but the reasons for this are not clear. It is possible that some optical effect causes light to be bent round the lower parts of the meniscus. An alternative explanation for lack of contrast towards the lower part of the meniscus may be vibration of the liquid interface from external sources although this was never observed visually. Nevertheless, it is felt that such deviations between theory and experiment that exist do not invalidate the generality of the computation described in the paper.

Furthermore, there is no reason to suspect that other fluids will deviate from the predicted values, unless they deviate from the assumptions of perfect wetting or zero contact angles.

The main contribution of this work has been the presentation of a calculation of meniscus profiles on the outside of circular wires. The calculation has enabled the maximum height (B) and the curvature at the highest point (C) to be given as a function of G_0 [equations (19) and (20)]. The validity of the computation has been verified by experiment for $0{\cdot}2 < G_0 < 1{\cdot}7$, which is within the region of technological importance of $0{\cdot}03 < G_0 < 3$. Due to the greater importance of the $1/G_0$ term in equation (20) at low G_0, it is felt that equation (20) will be valid right down to $G_0 \rightarrow 0$; and that any errors in B will not greatly affect the estimation of C_E. The work is limited to menisci of liquids which wet the surface perfectly and have a contact angle of zero, and which have surfaces free of surface active impurities.

The work was supported by a fellowship from the Standard Oil Co. of California and by Grant G-19820 from the U.S. National Science Foundation. The authors would like to thank Mr Jack Whitehead for his help.

REFERENCES

ADAM, N. K. 1938 *The Physics and Chemistry of Surfaces*, chap. 9. Oxford: Clarendon Press.

BONDARENKO, V. S. 1948 *Trud. Groznyy. Neft. Inst.*, Article Collection, no. 3, p. 133.

HAMMING, R. W. 1962 *Numerical Methods for Engineers and Scientists*. New York: McGraw Hill.

GUTFINGER, C. & TALLMADGE, J. A. 1964 *Amer. Inst. Chem. Engrs Journal*, **10**, 774.

LANDAU, L. D. & LEVICH, V. G. 1942 *Acta Physiochemica U.R.S.S.*, **17**, 41.

LANDAU, L. D. & LIFSHITZ, E. M. 1959 *Fluid Mechanics*, p. 235. New York: Pergamon Press.

LANGE, N. A. (ed.) 1961 *Handbook of Chemistry*. Sandusky, Ohio: Handbook Publ. Inc.

LEVICH, V. G. 1962 *Physicochemical Hydrodynamics*, p. 379. New York: Prentice Hall.

TALLMADGE J. A., LABINE, R. A. & WOOD, B. H. 1965 *Ind. Enging. Chem. Fund.* **4**, in press.

VAN ROSSUM, J. J. 1958 *Appl. Sci. Res.* A, **7**, 121.

WHITE, D. A. 1965 Ph.D. Dissertation, Dept. of Engng. and Applied Science, Yale University.